

## **CHAPTER III**

### **EXPERIMENTAL**

#### **3.1 Materials**

##### **3.1.1 Gases**

Gases used in this research work were:

- 24.85% carbon monoxides in helium from Thai Industrial Gases Public Company Limited.
- 8% oxygen in helium from Thai Industrial Gases Public Company Limited.
- High purity oxygen (99.7%) from Praxair (Thailand) Company Limited.
- Ultra high purity hydrogen (99.999%) from Thai Industrial Gases Public Company Limited.
- 20% carbon dioxide in helium from Praxair (Thailand) Company Limited.
- High purity helium (99.99%) from Thai Industrial Gases Public Company Limited.
- Ultra high purity helium (99.999%) from Thai Industrial Gases Public Company Limited.
- High purity nitrogen (99.99%) from Thai Industrial Gases Public Company Limited.

##### **3.1.2 Chemicals**

Catalyst preparation required the following chemicals:

- Sodium carbonate anhydrous ( $\text{Na}_2\text{CO}_3$ ) from Riedel-de Haen.
- Hydrogen tetrachloroaurate (III) ( $\text{HAuCl}_4 \cdot x\text{H}_2\text{O}$ ), 99.9%, Au 49.46% from Alfa AESAR, a Johnson Matthey Company.
- Manganese (II) nitrate hexahydrate 98% ( $\text{Mn}(\text{NO}_3)_2 \cdot 6\text{H}_2\text{O}$ ) from Aldrich Chemical Company, Inc.

- Ferric (III) nitrate nonahydrate ( $\text{Fe}(\text{NO}_3)_3 \cdot 9\text{H}_2\text{O}$ ) from ACS Xenon.

- Hydrochloric acid 35.4% (HCl) from BDH Laboratory Supplies.
- Nitric acid 65% ( $\text{HNO}_3$ ) from Riedel-deHaen.
- Gold standard solution for AAS from Fluka Chemie.

## 3.2 Equipment

The experiment system had 3 main parts as shown in Figure 3.1.

### 3.2.1 Gas Blending System

The reactant gas consisted of CO, H<sub>2</sub>, O<sub>2</sub>, and CO<sub>2</sub> balanced in He. Firstly, each stream was passed through a micron filter in order to remove particles and then check valve to prevent reverse flow. After that, the flow rates were controlled by 840 Sierra Instruments model mass flow controllers in order to achieve the desired concentrations. All of the streams were mixed in the mixer and passed through the water bath to be humidified before going into the reactor.

### 3.2.2 Catalytic Reactor

The selective CO oxidation was carried out in a Pyrex glass U-tube micro-reactor with an inside diameter of 4 mm at atmospheric pressure. In the middle of the reactor was the catalyst packed in between glass wool plugs. The temperature of the catalyst bed was controlled and monitored by PID temperature controller equipped with a chromel-alumel thermocouple (type K).

### 3.2.3 Analytical Instrumentation

The effluent gas from the reactor was passed through the drierite to trap water before being qualitatively and quantitatively analyzed by autosampling with a Hewlett Packard 5890 series II gas chromatograph with thermal conductivity detector. The column in this chromatograph was carbosphere, 80/100 mesh, and 10 ft x 1/8-inch stainless steel packed column. Carrier gas was ultra high purity helium

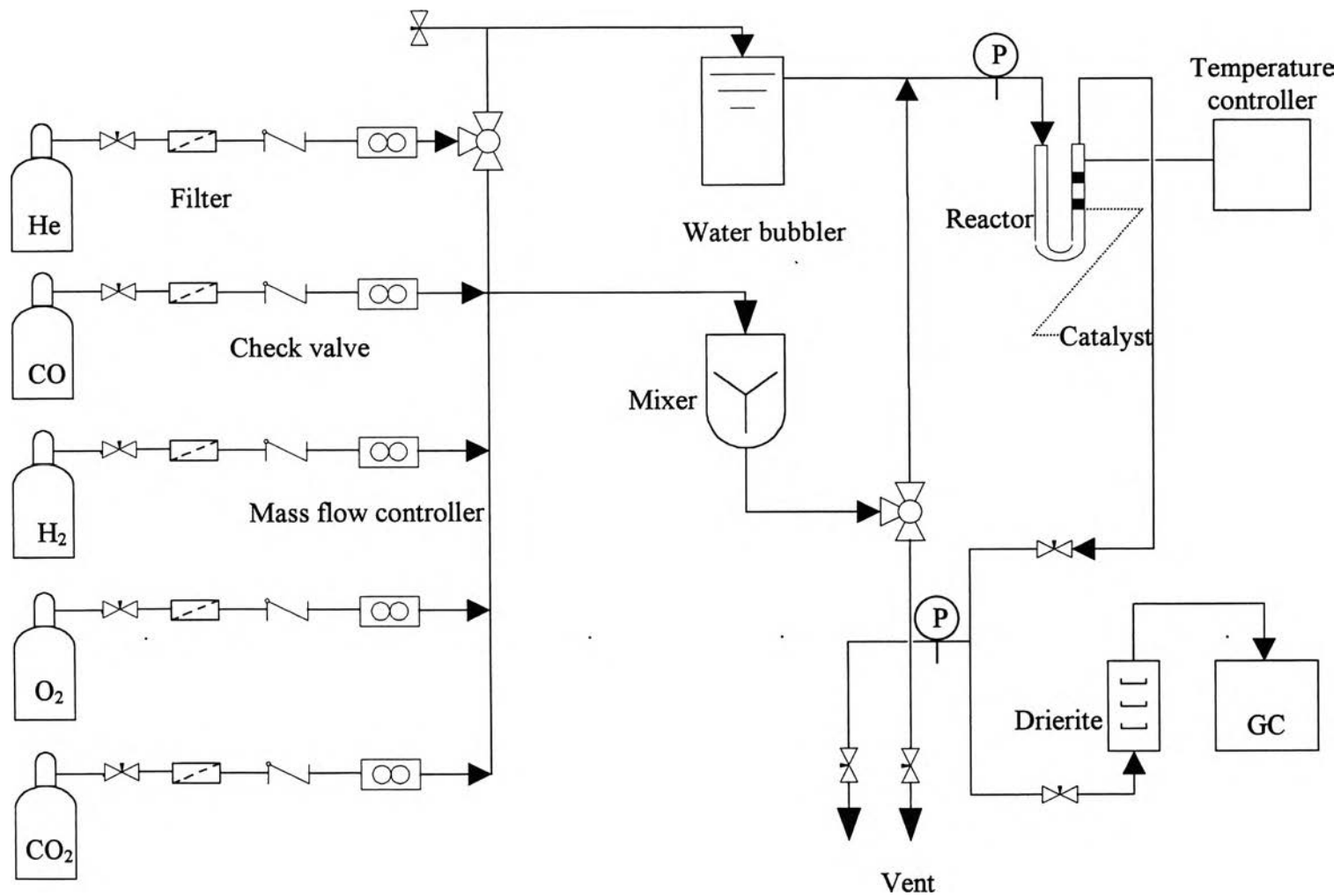


**Figure 3.1** The schematic flow diagram of experimental set-up.

with the flow rate of 32 ml/min. The temperature of the injector, oven and detector were 110, 55 and 175°C, respectively. The output of the chromatograph was recorded by a Hewlett Packard 3365 series II chemstation. For the qualitative analysis, the observed peaks were identified by comparison with the retention time of the standard gases; and for the quantitative analysis, peak area was used to determine the composition of the outlet gas based on the calibration curves obtained from known composition gases.

### **3.3 Catalyst Preparation Procedure**

Co-precipitation was used for catalyst preparation. An aqueous solution of 1 M Na<sub>2</sub>CO<sub>3</sub> was added dropwise into an aqueous mixture of 0.1 M Mn(NO<sub>3</sub>)<sub>2</sub> or 0.1 M Fe(NO<sub>3</sub>)<sub>3</sub> and 0.1 M HAuCl<sub>4</sub> under vigorous stirring condition at 80°C. The mixture was kept at a pH of 8 for 1 h. The precipitate was separated out from solution by centrifuge at 2,000 rpm for 5 min. Excess ions were eliminated by washing with warm deionized water. Deionized precipitate was dried at 110°C overnight and calcined for 2 h. After calcination the powder was ground and sieved to 80-120 mesh size and kept in a desiccator.

### **3.4 Catalyst Characterization**

To understand the effect of preparation parameters over the properties and the activities of catalysts, it was necessary to conduct some characterizations. In this work, several characterizations were utilized.

#### **3.4.1 BET Surface Area Measurement**

One of the most important properties of a heterogeneous catalyst is its surface area since the reaction takes place on the catalyst surface. The determination of surface area and pore size was done using the Autosorb-1 Gas Sorption System (Quantachrome Corporation). This equipment is based on Brunauer-Emmett-Teller (BET) method. N<sub>2</sub> gas with cross-sectional area of  $16.2 \times 10^{-20}$  m<sup>2</sup>/molecule was used as the adsorbate at liquid nitrogen temperature of 77 K. Before measurement,

sample was outgassed by heating under vacuum at 150°C for 2 h to eliminate adsorbed species at the surface. Twenty-one point adsorption isotherms at  $P/P_0$  ratio less than 1 was utilized to obtain the surface area. The result was analyzed by Autosorb Anygas Software Version 2.1, which were calculated using the BET equation as shown in Equation 3.1.

$$\frac{1}{W \times \left( \frac{P_0}{P} - 1 \right)} = \frac{1}{W_m \times C} + \frac{(C-1)}{(W_m \times C)} \times \left( \frac{P}{P_0} \right) \quad (3.1)$$

where:

- P = pressure of gas
- $P_0$  = saturated vapor pressure of the liquid at the operating temperature
- W = weight of gas adsorbed at a relative pressure  $P_0$
- $W_m$  = weight of adsorbate constituting a monolayer of surface coverage
- C = constant that is related to the energy of adsorption in the first adsorbed layer and magnitude of the adsorbent/adsorbate interaction.

The surface area was calculated by Equation 3.2.

$$S = \frac{W_m \times A_{\text{nitrogen}} \times (6.02 \times 10^{23})}{M_{w, \text{nitrogen}}} \quad (3.2)$$

where:

- S = specific surface area ( $\text{m}^2/\text{g}$ )
- $A_{\text{nitrogen}}$  = cross-sectionnal area of one molecule  $\text{N}_2$   
= 0.162  $\text{nm}^2$  (at 77 K)
- $M_{w, \text{nitrogen}}$  = molecular weight of  $\text{N}_2$ , 28

### 3.4.2 X-Ray Diffraction (XRD)

The crystalline structure of oxide supports and the mean particle diameter of Au were analyzed by means of a Rigaku X-Ray diffractometer system (RINT-2200) with Cu tube for generating  $\text{CuK}_\alpha$  radiation (1.5406 Å) and nickel filter. It is also possible to achieve a relative quantitative analysis by the intensity of the peak. For the same crystalline substance the higher of the peak indicates the higher content of that phase.

RINT-2200 was used to obtain XRD pattern at a generator voltage of 40 kV and a generator current of 30 mA. The goniometer parameters were divergence slit =  $1^\circ$  ( $2\theta$ ); scattering slit =  $1^\circ$  ( $2\theta$ ); and receiving slit = 0.3 mm. The scan speed of  $5^\circ$  ( $2\theta$ )/min with scan step of 0.02 ( $2\theta$ ) was used for the continuous run in  $5$  to  $90^\circ$  ( $2\theta$ ) range. Sample should be ground to a fine homogenous powder and held in a beam in a thin-walled glass container. The signal was sent to an on-line computer to record and analyze. Scherrer equation in the form of Equation 3.3 shows the relationship between the crystalline thickness ( $D_b$ ) and the broadening ( $\beta$ ) of the diffraction line corresponding to the Bragg angle ( $\theta$ ) using wavelength ( $\lambda$ ).

$$D_b = \frac{K \times \lambda}{B_d \times \cos\theta} \quad (3.3)$$

where:

$D_b$  = mean crystalline diameter (Å)

$K$  = Scherrer constant, 0.9

$\lambda$  = X-Ray wave length (Å)

$B_d$  = angular width of peak in term of  $\Delta$  ( $2\theta$ ) (radian)

$\theta$  = Bragg angle of the reflection (degree)

It is important to note here that the result from the Scherrer Equation is a crystallite thickness that is perpendicular to the diffraction planes rather than an actual particle size. It is necessary to apply a correction factor that depends on the actual shape of the crystallites and on the Millers indices of the diffracting planes in

order to obtain the actual crystallite size from the thickness. Correction factors are given in Table 3.1 for some common geometries (Lemaitre *et al.*, 1984).

**Table 3.1** Values of the geometric factor ( $g$ ), such as  $d = gD_b$

Geometry of the crystallite	$g$	Definition of $d$
Sphere	4/3	Diameter
Hemisphere	8/3	Diameter

XRD can also give some information on the dispersion of a supported catalyst only if it is in the form of a separate crystallite phase.

#### 3.4.3 Atomic Absorption Spectroscopy (AAS)

The content of Au (atomic ratio) in prepared catalyst was known from the preparation procedure. However, it is necessary to determine the actual one since Au might be lost during the preparation steps leading to the smaller amount of Au compare to the calculated amount. The AAS, VARIAN model 300/400 was utilized to determine the actual percent Au loading on supports. A known weight amount of catalyst was dissolved in aqua regia solution composed of hydrochloric acid and nitric acid with a ratio of 82:18 and then heated to 100°C for one hour. Several standard solutions were made from stock solution of 1,000 ppm to establish a calibration curve. By measuring the absorbance of the prepared solution the amount of Au loaded on the supports were obtained.

#### 3.4.4 Transmission Electron Microscopy (TEM)

The most widespread application of transmission electron microscopy in catalytic research is in measurement of size distributions of supported particles in order to determine from it the dispersion of the (usually) active phase. In this work, TEM was used to investigate the average crystallite size of Au. This information is very important to the catalyst activity because Bethke *et al.* (2000) confirmed that an optimal average Au particle size of about 5-10 nm gave the best activity and

selectivity. The TEM was carried out using a JEM 2010 operating at 200 kV in bright and dark field modes. More or less parallel electron beam uniformly irradiated the part of the studied specimen. The transmitted beam was focused by the objective lens and then propagated through several subsequent lenses. Diffraction pattern and the image of the specimen were observed from selected area. The way to prepare catalysts in a thin form suitable for TEM is to crush and grind the samples in a mortar. The fine powder thus obtained was dispersed in ethanol by use of an ultrasonic bath, and a drop of the suspension was deposited on a thin carbon film supported on a standard electron microscope grid. Image processing for contrast enhancement and image evaluation were done by means of the programs Digital Micrograph.

#### 3.4.5 Thermal Gravity Analysis (TGA)

Thermal Gravity Analysis (TGA) technique was used to determine the phase change of supports using the Du Pont TGA 2950 Thermogravimetric Analyzer. The catalysts were first exposed to a continuous flow of nitrogen (as a protective gas) and air (as a purge gas) at a flow rate of 10 and 20 ml/min, respectively. Then, by applying a temperature program from 30°C to 700°C with a heating rate of 10°C/min the mass changes of catalysts were monitored and recorded by the TGA instrument thermal analyst system. The purge gas was used to prevent back diffusion of the evolved gases from the operation. Heating rate and sample temperature were measured by the thermocouple located above the sample.

### 3.5 Activity Measurement

The reaction was carried out in the fixed bed reactor described previously packed with 100 mg catalyst of 80-120 mesh in size. The feed gas contained 1% CO, 2% CO<sub>2</sub>, 1% O<sub>2</sub>, 2.6% H<sub>2</sub>O and 40% H<sub>2</sub> balanced in He passing through the catalyst bed at the total flow rate of 50 ml/min (SV=30,000 mlg<sup>-1</sup>h<sup>-1</sup>) at atmospheric pressure.



### 3.5.1 Effect of Catalyst Pretreatment

Pretreatment may cause some changes in the structure of the catalyst leading to the changes in the activity and selectivity.

Three catalyst pretreatment procedures were used to see the effect on the catalyst activity.

- Sample was heated to 200°C and kept there for 2 h by 50 ml/min of He flow, then cooled down to the reaction temperature.
- Sample was heated to 200°C and kept there for 2 h by 50 ml/min of 10% H<sub>2</sub> in He flow, then cooled down to the reaction temperature.
- Sample was heated to 200°C and kept there for 2 h by 50 ml/min of 10% O<sub>2</sub> in He flow, then cooled down to the reaction temperature.

### 3.5.2 Effect of Calcination Temperature

In the preparation procedure, calcination was the last step to form the catalyst structure. Different calcination temperatures formed the difference in catalyst morphology with different activities.

The calcination temperature was differently varied with different kinds of catalysts. For Au/MnO<sub>x</sub>, 200 and 300°C for 2 h were used to investigate the effect of calcination temperature while 300 and 400°C were used for Au/FeO<sub>x</sub> instead.

### 3.5.3 Effect of Au Loading

Haruta *et al.* (1993) found that the reaction solely takes place on the Au/oxide perimeter with CO adsorbed on Au and O<sub>2</sub> originated from oxide support. Thus, the amount of Au loaded onto the catalyst must have the effect on the catalyst activity. In this work atomic ratio was used for Au loading. The appropriate atomic ratios investigated for Au/MnO<sub>x</sub> and Au/Fe<sub>2</sub>O<sub>3</sub> were 1/30, 1/60, and 1/120.

### 3.5.4 Effect of CO<sub>2</sub> Concentration in the Feed Gas

Hoflund *et al.* (1995) found that CO<sub>2</sub> in the reactant gas mixture adversely affect the behavior of catalyst due to CO<sub>2</sub> retention on their surfaces.

Thus, this work attempted to prove that idea by studying the catalyst activity at different concentrations of CO<sub>2</sub> in the feed gas that were 0% and 10%.

### 3.5.5 Effect of H<sub>2</sub>O Concentration in the Feed Gas

Normally, catalyst activity is depressed by the presence of H<sub>2</sub>O. However, in the case of Au/MnO<sub>x</sub>, the catalyst activity is enhanced by moisture (Torres Sanchez *et al.*, 1997). To make it clear, the effect of water was carried out by cutting off the water in feed gas.

### 3.5.6 Deactivation Test

Once the best catalyst was determined, it was necessary to check whether it would last long or not in order to be commercially usable. Deactivation test was carried out for 48 h.

## 3.6 Calculation

The conversion and selectivity were calculated by Equations 3.4 and 3.5, respectively.

$$X = \frac{[\text{CO}]_0 - [\text{CO}]}{[\text{CO}]_0} \times 100 \quad (3.4)$$

$$S = \frac{[\text{O}_2]_{\text{CO}}}{[\text{O}_2]_{\text{CO}} + [\text{O}_2]_{\text{H}_2}} \times 100 \quad (3.5)$$

where:

X = CO conversion (%)

S = selectivity (%)

[O<sub>2</sub>]<sub>CO</sub> = amount of O<sub>2</sub> for CO oxidation only

[O<sub>2</sub>]<sub>H<sub>2</sub></sub> = amount of O<sub>2</sub> for H<sub>2</sub> oxidation only

[CO]<sub>0</sub> = concentration of CO in the reactant gas

[CO] = concentration of CO in the product gas

### 3.7 Experimental Plan

Catalyst	: 100 mg of 80-120 mesh size
Reactant gas	: 1% CO, 1% O <sub>2</sub> , 2% CO <sub>2</sub> , 2.6% H <sub>2</sub> O and 40% H <sub>2</sub> balanced in He
Flow rate	: 50 ml/min
Space velocity	: 30,000 mlg <sup>-1</sup> h <sup>-1</sup>
Reaction temperature	: 50-190°C
Reaction pressure	: atmospheric pressure

Two types of catalyst, which are Au/MnO<sub>x</sub> and Au/FeO<sub>x</sub> were taken into the consideration in this work. The whole picture can be seen in Table 3.2.

The experimental plan can be divided into three parts. Firstly, it was needed to investigate the operating condition for both catalysts. Three parameters were considered, which are pretreatment condition, calcination temperature and atomic ratio (Au/Mn or Au/Fe). For each parameter, in order to see its effect, the others two were fixed. After finding out the best condition for that parameter, that was chosen for the next step to look for the next ones. Finally, the optimum operating condition was obtained. For example, when pretreatment condition was investigated, the calcination temperature and atomic ratio were fixed at 200°C and 1/120 for Au/MnO<sub>x</sub>, respectively. As the result, He was the best pretreatment condition as compared to O<sub>2</sub> or H<sub>2</sub>. Then, He pretreatment was utilized afterward for looking at the next parameters.

Secondly, the effect of CO<sub>2</sub> and H<sub>2</sub>O in the feed gas on catalyst activity was determined. By comparing the activity difference between with and with out CO<sub>2</sub> or H<sub>2</sub>O, it can be cleared.

Lastly, the catalyst deactivation test was taken for 48 h in order to make sure that catalyst activity could last for that long.

**Table 3.2** Experimental plan

	Catalyst type	Pretreatment condition	Calcination temperature (°C)	Atomic ratio	Run no.
Effect of pretreatment condition	Au/MnO <sub>x</sub>	He	200	1/120	1
		O <sub>2</sub>	200	1/120	2
		H <sub>2</sub>	200	1/120	3
	Au/FeO <sub>x</sub>	He	400	1/60	4
		O <sub>2</sub>	400	1/60	5
		H <sub>2</sub>	400	1/60	6
Effect of calcination temperature	Au/MnO <sub>x</sub>	He	200	1/120	-
		He	300	1/120	7
	Au/FeO <sub>x</sub>	O <sub>2</sub>	300	1/30	8
		O <sub>2</sub>	400	1/30	9
Effect of atomic ratio	Au/MnO <sub>x</sub>	He	300	1/120	-
		He	300	1/60	10
		He	300	1/30	11
	Au/FeO <sub>x</sub>	O <sub>2</sub>	400	1/120	12
		O <sub>2</sub>	400	1/60	-
		O <sub>2</sub>	400	1/30	-
Effect of CO <sub>2</sub>	Au/MnO <sub>x</sub>	He	300	1/30	13
	Au/FeO <sub>x</sub>	O <sub>2</sub>	400	1/30	14
Effect of H <sub>2</sub> O	Au/MnO <sub>x</sub>	He	300	1/30	15
	Au/FeO <sub>x</sub>	O <sub>2</sub>	400	1/30	16
Deactivation test	Au/MnO <sub>x</sub>	He	300	1/30	17
	Au/FeO <sub>x</sub>	O <sub>2</sub>	400	1/30	18

### 3.7.1 Effect of Catalyst Pretreatment

**Table 3.3** Experimental plan for effect of catalyst pretreatment

Run no.	Catalyst type	Calcination temperature (°C)	Atomic ratio	Pretreatment		
				He	H <sub>2</sub>	O <sub>2</sub>
1-3	Au/MnO <sub>x</sub>	200	1/120	√	√	√
4-6	Au/FeO <sub>x</sub>	400	1/60	√	√	√

### 3.7.2 Effect of Calcination Temperature

**Table 3.4** Experimental plan for effect of calcination temperature

Run no.	Type of catalyst	Pretreatment	Atomic ratio	Calcination temperature (°C)		
				200	300	400
7	Au/MnO <sub>x</sub>	He	1/120	√*	√	-
8-9	Au/FeO <sub>x</sub>	O <sub>2</sub>	1/60	-	√	√

\* : The run was counted previously

### 3.7.3 Effect of Au Loading

**Table 3.5** Experimental plan for effect of Au loading

Run no.	Catalyst type	Pretreatment	Calcination temperature (°C)	Atomic ratio		
				1/120	1/60	1/30
10-11	Au/MnO <sub>x</sub>	He	300	√*	√	√
12	Au/FeO <sub>x</sub>	O <sub>2</sub>	400	√	√*	√*

### 3.7.4 Effect of CO<sub>2</sub> in the Feed Gas

**Table 3.6** Experimental plan for effect of CO<sub>2</sub> in the feed gas

Run no.	Catalyst type	Pretreatment	Calcination temperature (°C)	Atom.ratio	[CO <sub>2</sub> ] (%)	
					10	0
13	Au/MnO <sub>x</sub>	He	300	1/30	√	√
14	Au/FeO <sub>x</sub>	O <sub>2</sub>	400	1/30	√	√

### 3.7.5 Effect of H<sub>2</sub>O in the Feed Gas

**Table 3.7** Experimental plan for effect of H<sub>2</sub>O in the feed gas

Run no.	Catalyst type	Pretreatment	Calcination temperature (°C)	Atom.ratio	[H <sub>2</sub> O] (%)	
					10	0
15	Au/MnO <sub>x</sub>	He	300	1/30	√	√
16	Au/FeO <sub>x</sub>	O <sub>2</sub>	400	1/30	√	√

### 3.7.6 Deactivation Test

**Table 3.8** Experimental plan for the deactivation test

Run no.	Catalyst type	Pretreatment	Calcination temperature (°C)	Atomic ratio	Tested time (h)
					48
17	Au/MnO <sub>x</sub>	He	300	1/30	√
18	Au/FeO <sub>x</sub>	O <sub>2</sub>	400	1/30	√